

Band offsets between Si and epitaxial rare earth sesquioxides (RE 2 O 3 , RE = La , Nd , Gd , Lu) : Effect of 4 f -shell occupancy

V. V. Afanas'ev, M. Badylevich, A. Stesmans, A. Laha, H. J. Osten, A. Fissel, W. Tian, L. F. Edge, and D. G. Schlom

Citation: *Applied Physics Letters* **93**, 192105 (2008); doi: 10.1063/1.3003872

View online: <http://dx.doi.org/10.1063/1.3003872>

View Table of Contents: <http://scitation.aip.org/content/aip/journal/apl/93/19?ver=pdfcov>

Published by the *AIP Publishing*

Articles you may be interested in

[Effects of Al doping and annealing on chemical states and band diagram of Y 2 O 3 /Si gate stacks studied by photoemission and x-ray absorption spectroscopy](#)

J. Vac. Sci. Technol. A **28**, 16 (2010); 10.1116/1.3259869

[Band offsets of Er 2 O 3 films epitaxially grown on Si substrates](#)

Appl. Phys. Lett. **88**, 162909 (2006); 10.1063/1.2196476

[Band alignment at the interface of \(100 \) Si with Hf x Ta 1 - x O y high- κ dielectric layers](#)

Appl. Phys. Lett. **86**, 072108 (2005); 10.1063/1.1866640

[First principles investigation of scaling trends of zirconium silicate interface band offsets](#)

J. Appl. Phys. **90**, 1333 (2001); 10.1063/1.1378338

[Band offset and structure of SrTiO 3 / Si \(001\) heterojunctions](#)

J. Vac. Sci. Technol. A **19**, 934 (2001); 10.1116/1.1365132



You don't still use this cell phone

or this computer

Why are you still using an AFM designed in the 80's?

It is time to upgrade your AFM

Minimum \$20,000 trade-in discount for purchases before August 31st

Asylum Research is today's technology leader in AFM

dropmyoldAFM@oxinst.com

OXFORD INSTRUMENTS
The Business of Science®

Band offsets between Si and epitaxial rare earth sesquioxides (RE₂O₃, RE=La, Nd, Gd, Lu): Effect of 4f-shell occupancy

V. V. Afanas'ev,^{1,a)} M. Badylevich,¹ A. Stesmans,¹ A. Laha,² H. J. Osten,² A. Fissel,³ W. Tian,⁴ L. F. Edge,⁴ and D. G. Schlom⁴

¹Department of Physics and Astronomy and INPAC-Institute for Nanoscale Physics and Chemistry, University of Leuven, Celestijnenlaan 200D, B-3001 Leuven, Belgium

²Institute of Electronic Materials and Devices, Leibniz University of Hannover, Appelstrasse 11A, D-30167 Hannover, Germany

³Information Technology Laboratory, Leibniz University of Hannover, Schneiderberg 32, D-30167 Hannover, Germany

⁴Department of Materials Science and Engineering and Materials Research Institute, Cornell University, Ithaca, New York 14853-1501, USA

(Received 9 July 2008; accepted 27 September 2008; published online 11 November 2008)

Internal photoemission of electrons and holes into cubic Nd₂O₃ epitaxially grown on (100)Si reveals a significant contribution of Nd 4f states to the spectrum of the oxide gap states. In contrast to oxides of other rare earth (RE) elements (Gd, Lu) epitaxially grown in the same cubic polymorph, to hexagonal LaLuO₃, and to polycrystalline HfO₂, the occupied Nd 4f states produce an additional filled band 0.8 eV above the O 2p derived valence band. The unoccupied portion of the Nd 4f shell leads to empty electron states in the energy range of 1 eV below the RE 5d derived oxide conduction band. The exposed Nd 4f states suggest the possibility to use this metal and, possibly, other REs with low f-shell occupancy to control the interface band offsets by selective interface doping. © 2008 American Institute of Physics. [DOI: 10.1063/1.3003872]

Insulating oxides of rare earths (REs), particularly the sesquioxides RE₂O₃, are attracting attention as dielectric materials suitable for replacing SiO₂ in microelectronic devices because they combine the best features of candidate insulators including high dielectric permittivity (κ), wide bandgap, and thermodynamic stability.¹ In addition, thanks to significant variation of the molar volume from La to Lu oxides (about 20% decrease, “lanthanide contraction”^{2,3}), their lattice parameter can be selected to enable epitaxial growth on the surface of crystalline semiconductors. What still remains unclear is the role of the partially occupied 4f states of the RE cations in determining the barriers for electrons and holes. It was found for thin layers of amorphous or polycrystalline heavy RE sesquioxides (Gd, Dy, and Lu), several RE scandates (LaScO₃, DyScO₃, and GdScO₃), LaAlO₃, and LaLuO₃ that the occupancy of the 4f shell has only a marginal influence on the band alignment with Si or Ge.^{4–10} The conduction band (CB) and valence band (VB) offsets at these interfaces appear to be close to those at the interfaces of the same semiconductors with HfO₂ in which the 4f shell is filled.¹¹ In the case of low f-shell occupancy, however, the splitting between occupied and empty f-states is expected to decrease¹² causing the sesquioxide gap narrowing.^{3,13,14} Optical measurements indicate significant gap narrowing in light RE sesquioxides (Pr, Nd, Sm, and Eu), which is ascribed to the occupied 4f states lying energetically above the O 2p states in the oxide VB.¹⁵ By contrast, the presence of unoccupied f-states in the upper portion of the gap was suggested to narrow the gap in Nd₂O₃.¹⁶ The important factor affecting the energy position of RE 4f states is known to be the crystal field splitting,¹⁷ making this portion of the electron spectrum sensitive to the oxide crystal phase. Oxides of

light REs (La, Pr, and Nd) usually crystallize in the hexagonal phase, while heavy RE sesquioxide crystals have the cubic Mn₂O₃ (bixbyite) structure^{18,19} making meaningful comparison between bulk the phase(s) of different RE sesquioxides difficult. In the present work, this problem is resolved by growing cubic (bixbyite) RE oxides epitaxially on atomically clean Si crystal surfaces. While not observed for Gd₂O₃, Lu₂O₃, Lu₂O₃, and HfO₂, we reveal the f-shell contribution to the density of states (DOS) in Nd₂O₃ by analysing the oxide CB and VB edges separately using internal photoemission (IPE) of electrons and holes from Si.

Two Si surface orientations were used to enable the epitaxial growth: (100) for Nd₂O₃ and Gd₂O₃ and (111) for Gd₂O₃ and Lu₂O₃. The growth was performed at 650–700 °C by evaporating the source material under a low background pressure of oxygen resulting in abrupt (i.e., SiO₂-free) Si/RE oxide interfaces.^{20,21} Earlier comparison of Gd₂O₃ epilayers on (100) and (111)Si faces indicated the same band alignment between Si and the oxide,¹⁰ thus allowing a direct comparison among the studied sample series. To investigate the possible effect of unoccupied states of La on the oxide and interface DOS, epitaxial LaLuO₃ films were grown on (111)Si. This composition allowed us to reduce the chemical interaction of La with ambient moisture known to occur at room temperature.²² The resulting epitaxial LaLuO₃/(111)Si films are found to crystallize as a hexagonal La₂O₃–Lu₂O₃ solid solution structure rather than the perovskite structure. Nevertheless, the band offsets at the interface between hexagonal LaLuO₃ and Si appear to be the same as in the amorphous LaLuO₃/(100)Si studied earlier,^{9,11} suggesting only a weak sensitivity of the O 2p-RE 5d gap to the structure of the oxide. For the sake of comparison to the case of a filled 4f shell, polycrystalline HfO₂ layers containing tetragonal and monoclinic phases were deposited at 485 °C from metallo-organic precursor on (100)Si

^{a)}Electronic mail: valeri.afanasiev@fys.kuleuven.be.

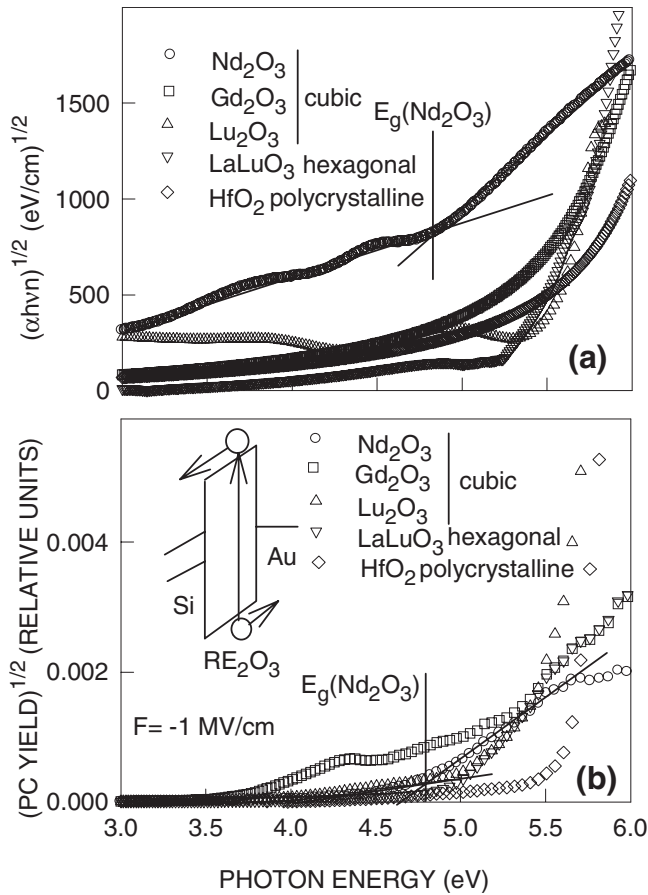


FIG. 1. (a) Square root of the optical absorption coefficient α (normalized to the photon energy $h\nu$ and refractive index n) as a function of photon energy derived from SE data for the RE oxides and HfO_2 studied. Lines indicate linear fits to extract the bandgap E_g of Nd_2O_3 . (b) Square root of the PC quantum yield as a function of photon energy measured on different oxides under an externally applied electric field F of -1 MV/cm (cf. the band diagram in the inset). Lines indicate linear fits to determine the bandgap E_g of Nd_2O_3 .

substrates covered with a 0.8-nm-thick chemical oxide. The thickness of the oxide layers was in the range between 4 and 40 nm as determined using x-ray reflectivity and spectroscopic ellipsometry (SE) measurements. Capacitor structures were fabricated by thermoresistive evaporation of 0.5 nm² semitransparent (15-nm-thick) Au or Al electrodes onto the oxide. These were used in IPE and photoconductivity (PC) room temperature experiments.¹¹ The quantum yield Y was defined as the photocurrent normalized to the incident photon flux and analysed in the photon energy ($h\nu$) range of 2–6.5 eV with constant spectral resolution of 2 nm. By considering the IPE of electrons and holes from Si into different insulators, the initial energy distribution of photoexcited charge carriers in Si is the same for all samples. Therefore, the observed differences in the IPE spectra will reflect the different energy distribution of the DOS over the insulating collector layers studied.²³

Panels (a) and (b) in Fig. 1 exemplify the spectral dependences of the normalized optical absorption coefficient (α) determined by fitting the SE data and of the PC yield, respectively, for the insulating layers studied in the photon energy range close to the onset of intrinsic absorption. Compared to other oxides, Nd_2O_3 shows significantly enhanced absorption consistent with the smaller gap width observed in bulk crystals ($E_g \sim 4.7$ eV) as measured at 300 K (Ref. 15)

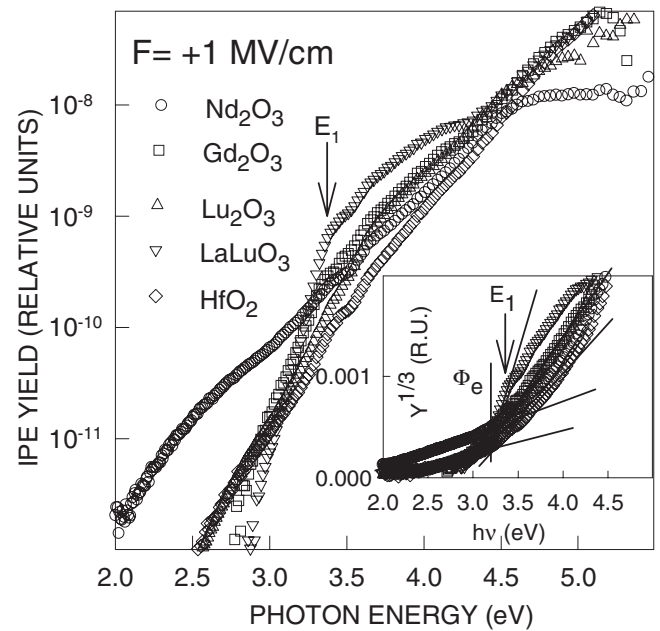


FIG. 2. Logarithmic spectral plots of the electron IPE quantum yield from Si into the CB of different RE oxides and HfO_2 measured under an externally applied electric field F of $+1$ MV/cm. The inset shows $Y^{1/3}$ - $h\nu$ plots used to determine the threshold Φ_e of electron IPE from the Si VB to the oxide CB. Arrow E_1 shows the energy of the Λ_3 - Λ_1 excitation in the Si crystal.

and 78 K.¹⁶ Using a linear fit of the $(\alpha h\nu)^{1/2}$ - $h\nu$ plot (n is the refractive index), indicated in Fig. 1(a) by lines, we obtain a similar bandgap $E_g = 4.8 \pm 0.1$ eV for the bixbyite Nd_2O_3 film. Although the same threshold can also be inferred from the PC spectral curves shown in panel (b), the PC quantum yield in Nd_2O_3 appears to be disproportionately low as compared to the strong optical absorption evident in (a). This observation indicates that most of the optical transitions involved in the optical absorption produce no free charge carriers, i.e., they are either of excitonic nature as occurs, for instance, in Y_2O_3 ,²⁴ or the electrons and holes are generated in strongly localized states facilitating efficient geminate recombination. To resolve this dilemma we performed IPE measurements which exclude the excitonic effects.

Logarithmic plots of electron and hole IPE yield as a function of $h\nu$ are shown in Fig. 2 (positive bias) and Fig. 3 (negative bias), respectively, with the bottom right inserts illustrating the determination of electron and hole IPE thresholds using $Y^{1/3}$ - $h\nu$ (Ref. 25) or $Y^{1/2}$ - $h\nu$ (Ref. 26) plots, respectively. As revealed by the electron IPE spectra presented in Fig. 2, (100)Si/ Nd_2O_3 shows greatly enhanced emission in the low ($h\nu < 3$ eV) energy range. As the density of interface traps derived from CV curves in the Nd_2O_3 samples is found to be in the same range as in Gd_2O_3 or Lu_2O_3 samples (of the order of 10^{12} cm⁻²), involvement of defect-assisted “pseudo-IPE” (Ref. 23) is unlikely to explain this enhancement of electron current. This conclusion is supported by the observation of the E_1 optical singularity at $h\nu = 3.4$ eV related to Λ_3 - Λ_1 excitation in silicon in all samples, pointing to the Si substrate as the source of the photoelectrons. Therefore, the cause of the IPE enhancement is associated with a downshift of the Nd_2O_3 CB bottom by approximately 1 eV. A second important observation is the smearing out of the IPE threshold associated with electron

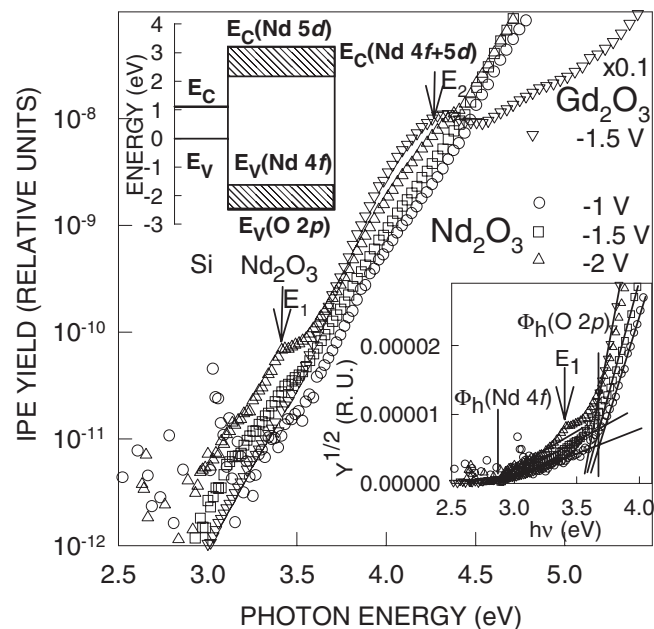


FIG. 3. Logarithmic spectral plots of the hole IPE quantum yield from (100)Si into the VB of Nd_2O_3 (19 nm) measured under different negative biases applied to the Au electrode. For comparison, the yield is also shown (scaled down by factor of 10) for the (100)Si/ Gd_2O_3 (11.2 nm)/Au structure. The bottom right inset shows $Y^{1/2}$ - $h\nu$ plots used to determine the threshold Φ_h of hole IPE from the Si CB to the oxide VB. The lines in the inset illustrate the determination of the IPE spectral thresholds. Arrows E_1 and E_2 mark the energy of Λ_3 - Λ_1 and X_4 - X_1/Σ_4 - Σ_1 excitations within the Si crystal, respectively. The top left insert shows schematic energy band diagram at the Si/ Nd_2O_3 interface inferred from the PC and IPE results. The energy scale is in measured with respect to the top of the Si VB. Shaded areas indicate the DOS components derived from the Nd 4f states.

IPE into the unoccupied RE 5d states in the (100)Si/ Nd_2O_3 structure, which constitute the lowest portion of CB in the other four oxides. This IPE threshold (indicated as Φ_e in the insert in Fig. 2) is found at around 3.1–3.2 eV at the interfaces of Gd_2O_3 , Lu_2O_3 , LaLuO_3 , and HfO_2 with Si,¹¹ but becomes less pronounced in Nd_2O_3 which might suggest hybridization of the Nd 5d and 4f states in its CB.

Hole IPE spectra, such as shown in Fig. 3 for different voltages applied to the Au electrode of (100)Si/ Nd_2O_3 (19 nm)/Au capacitors, indicate that in low electric fields the threshold of the hole IPE Φ_h is 3.7 ± 0.1 eV, which is close to that for the Gd_2O_3 case. With increasing negative bias voltage, however, the Nd_2O_3 sample develops a low-energy IPE tail stretching down to 2.9 ± 0.2 eV. The clear observation of the abovementioned E_1 optical singularity, marked by arrows in Fig. 3, suggests again Si as the source of the photoemitted holes. Apparently the IPE tail corresponds to hole injection into a band of occupied states lying approximately 0.8 eV above the O 2p derived VB top. As such an effect is not observed in any of the other RE sesquioxides studied or in HfO_2 , it is likely associated with occupied Nd 4f states which would also be in agreement with results obtained from photoelectron spectroscopy experiments.^{27,28} Accordingly, the observed hole IPE thresholds are identified in Fig. 3 as $\Phi_h(\text{O } 2p)$ and $\Phi_h(\text{Nd } 4f)$. The former threshold is seen at nearly the same energy in Nd_2O_3 as in Gd_2O_3 , Lu_2O_3 , or HfO_2 , suggesting

that the energy of the O 2p states is insensitive to the energy of the Nd 4f states. Thus, hybridization of these states is unlikely.

The energy band diagram at the Si/ Nd_2O_3 interface can now be compiled, as shown in the top left insert in Fig. 3 with contributions of Nd 4f states indicated by dashed regions. The latter allow one to reduce both the CB and VB offsets by nearly 1 eV, thus offering a method of interface barrier control by the introduction of a controlled amount of Nd into other RE sesquioxides. An obvious advantage inherent to this approach is that Nd is incorporated into the oxide structure as an isovalent substitution without necessarily forming dangling bonds or any other coordination defects.

The work done at KU Leuven was supported by the “Fonds voor Wetenschappelijk Onderzoek (FWO) Vlaanderen” through Grant No. 1.5.057.07.

- ¹See, e.g., D. G. Schlom and J. H. Haeni, *MRS Bull.* **27**, 198 (2002).
- ²N. Hirosaki, S. Ogata, and C. Kocer, *J. Alloys Compd.* **351**, 31 (2003).
- ³L. Petit, A. Svane, Z. Szotek, and W. M. Temmerman, *Phys. Rev. B* **72**, 205118 (2005).
- ⁴G. Seguini, E. Bonera, S. Spiga, G. Scarel, and M. Fanciulli, *Appl. Phys. Lett.* **85**, 5316 (2004).
- ⁵M. Perego, G. Seguini, G. Scarel, and M. Fanciulli, *Surf. Interface Anal.* **38**, 494 (2006).
- ⁶V. V. Afanas'ev, A. Stesmans, C. Zhao, M. Caymax, T. Heeg, J. Schubert, Y. Jia, D. G. Schlom, and G. Lucovsky, *Appl. Phys. Lett.* **85**, 5917 (2004).
- ⁷V. V. Afanas'ev, A. Stesmans, L. F. Edge, D. G. Schlom, T. Heeg, and J. Schubert, *Appl. Phys. Lett.* **88**, 032104 (2006).
- ⁸V. V. Afanas'ev, S. Shamulila, A. Stesmans, A. Dimoulas, Y. Panayiotatos, A. Sotiropoulos, M. Houssa, and D. P. Brunco, *Appl. Phys. Lett.* **88**, 132111 (2006).
- ⁹J. M. J. Lopes, M. Roeckrath, T. Heeg, E. Rije, J. Schubert, S. Mantl, V. V. Afanas'ev, S. Shamulila, A. Stesmans, Y. Jia, and D. G. Schlom, *Appl. Phys. Lett.* **89**, 222902 (2006).
- ¹⁰M. Badylevich, S. Shamulila, V. V. Afanas'ev, A. Stesmans, A. Laha, H. J. Osten, and A. Fissel, *Appl. Phys. Lett.* **90**, 252101 (2007).
- ¹¹V. V. Afanas'ev and A. Stesmans, *J. Appl. Phys.* **102**, 081301 (2007).
- ¹²F. Lopez-Aguilar and J. Costa-Quintana, *Phys. Status Solidi B* **118**, 779 (1983).
- ¹³M. Mikami and S. Nakamura, *J. Alloys Compd.* **408-412**, 687 (2006).
- ¹⁴N. Singh, S. M. Saini, T. Nautiyal, and S. Auluck, *J. Appl. Phys.* **100**, 083525 (2006).
- ¹⁵A. V. Prokofiev, A. I. Shelykh, and B. T. Melekh, *J. Alloys Compd.* **242**, 41 (1996).
- ¹⁶S. Kimura, F. Arai, and M. Ikezawa, *J. Phys. Soc. Jpn.* **69**, 3451 (2000).
- ¹⁷G. H. Dieke and H. M. Crosswhite, *Appl. Opt.* **2**, 675 (1963).
- ¹⁸*Numerical Data and Functional Relationships in Science and Technology*, edited by K.-H. Hellwege and A. M. Hellwege, Landolt-Börnstein, New Series, Group III, Vol. 7b (Springer, Berlin, 1975) p. 69.
- ¹⁹P. Villars and L. D. Calvert, *Pearson's Handbook of Crystallographic Data for Intermetallic Phases*, 2nd ed. (ASM International, Ohio, 1991).
- ²⁰A. Laha, H. J. Osten, and A. Fissel, *Appl. Phys. Lett.* **89**, 143514 (2006).
- ²¹A. Fissel, D. Kuhne, E. Bugiel, and H. J. Osten, *Appl. Phys. Lett.* **88**, 153105 (2006).
- ²²Y. Zhao, M. Toyama, K. Kita, K. Kyuno, and A. Toriumi, *Appl. Phys. Lett.* **88**, 072904 (2006).
- ²³V. V. Afanas'ev, *Internal Photoemission Spectroscopy: Principles and Applications* (Elsevier, Amsterdam, 2008).
- ²⁴T. Tomiki, T. Shikenbaru, Y. Ganaha, T. Futemma, H. Kato, M. Yuri, H. Fukutani, T. Miyahara, S. Shin, M. Ishigame, and J. Tamashiro, *J. Phys. Soc. Jpn.* **61**, 2951 (1992).
- ²⁵R. J. Powell, *J. Appl. Phys.* **41**, 2424 (1970).
- ²⁶J. S. Helman and F. Sanchez-Sinencio, *Phys. Rev. B* **7**, 3702 (1973).
- ²⁷M. V. Ryzhkov, V. A. Gubanov, Yu. A. Teterin, and A. S. Baev, *Z. Phys. B: Condens. Matter* **59**, 1 (1985).
- ²⁸F. Arai, S. Kimura, and M. Ikezawa, *J. Phys. Soc. Jpn.* **67**, 225 (1998).